

## Article

# Study on the Dispersion and Lubrication Properties of LDH in Lubricating Oil

Yong Li <sup>1,2</sup>, Qiang Zhang <sup>1</sup>, Weidong Zhou <sup>3</sup>, Yongwang Huang <sup>2</sup> and Jingbin Han <sup>1,\*</sup> 

<sup>1</sup> State Key Laboratory of Chemical Resource Engineering, Beijing University of Chemical Technology, Beijing 100029, China

<sup>2</sup> Tianjin Nisseki Lubricants & Grease Co., Ltd., Binhai New Area, Tianjin 300480, China

<sup>3</sup> State Key Laboratory of Engines, Tianjin University, Tianjin 300350, China

\* Correspondence: hanjb@mail.buct.edu.cn

**Abstract:** The dispersion of nanomaterials in lubricating oil plays an important role in the lubrication and wear-resistance properties. In this work, supramolecular layered double hydroxides (LDHs) were prepared and added to lubricating oil with different dispersants. The content of key elements in the samples was measured by an oil element analyzer, and the dispersion properties of different samples were studied. The friction coefficient of the samples was measured by high-frequency linear vibration (SRV), and the morphology and composition were characterized by SEM to study the antiwear performance and action mechanism of LDH. The oxidation induction time of the samples was measured by RBOT to study the antioxidygenic properties of LDH in lubricating oil. The results show that LDH can be well-dispersed in lubricating oil with the action of specific dispersants. After adding LDH, the antiwear performance of lubricating oil was improved, as a uniform and dense protective film was formed on the friction surface.

**Keywords:** layered double hydroxides; dispersant; lubricating oil; elemental analysis; friction and wear; friction mechanism

## 1. Introduction

Friction and wear are common in our daily life, and we often work with them in the field of tribology under a wide range of operating conditions [1]. However, unnecessary friction and wear may cause huge loss of raw materials and energy [2,3]. Worldwide, especially in highly industrialized countries, the losses caused by friction and wear of energy and materials are estimated to be as much as 5–7% of gross national product [4]. In order to solve these problems, lubricants are used in the fields of transportation [5], metal cutting [6], power generation [7], power transmission [8], etc. Among lubricants, mineral- and synthetic-based oils are most commonly used in industry due to their relatively high viscosity and pressure–viscosity coefficient [9]. They help to ensure that an elastohydrodynamic lubrication regime is formed by a sufficiently thick liquid film [10].

In the past few years, owing to their unique chemical and structural properties, a variety of nanomaterials have been used in oil to enhance its antifriction and antiwear properties [11]. Among them, owing to their high specific surface area and relatively weak interlayer (i.e., van der Waals) bond, two-dimensional (2D) layered materials such as molybdenum disulfide [12], tungsten disulfide [13] and multilayer graphene [14] are used as lubricating oil additives. The self-lubrication of these materials is mainly due to the interlaminar shear mechanism [15]. In each layer of the layered structure, the atoms are dense and strongly connected, while the layers are relatively far away, and the forces holding them together are relatively weak [16]. Strong interatomic bonding and packaging in each layer provide very high strength and toughness and reduce wear damage during sliding, and wide interlayer spacing and weak bonding ensure simple shearing or sliding [17]. Layered double hydroxides (LDHs) are a type of 2D nanomaterial [18]



**Citation:** Li, Y.; Zhang, Q.; Zhou, W.; Huang, Y.; Han, J. Study on the Dispersion and Lubrication Properties of LDH in Lubricating Oil. *Lubricants* **2023**, *11*, 147. <https://doi.org/10.3390/lubricants11030147>

Received: 2 February 2023

Revised: 11 March 2023

Accepted: 15 March 2023

Published: 19 March 2023



**Copyright:** © 2023 by the authors. Licensee MDPI, Basel, Switzerland. This article is an open access article distributed under the terms and conditions of the Creative Commons Attribution (CC BY) license (<https://creativecommons.org/licenses/by/4.0/>).

that possess good thermal stability compared with traditional layered materials [19], are non-toxic [20] and have a low production cost [21]. However, there are abundant hydroxyl groups [22] and a large number of unsaturated coordination structures [23] on the surface of the plate and at the edges of the sheets [24], making them difficult to disperse in lubricating oil and prone to sedimentation [25]. Thus, it is of great interest to explore the potential of LDH materials as lubricant additives. Zhao et al. [26] prepared MgAl-NO<sub>3</sub> LDHs and attempted to use an industrial surfactant, dodecanoic acid, as an intercalation anion to enhance their dispersion stability in oil. Wang et al. [27] synthesized a series of LDH nanomaterials with different chemical compositions and morphologies. Tribological tests show that during sliding, a dense and uniform friction film derived from LDH is formed on the sliding surface, which helps to reduce the coefficient of friction (COF) and improve antiwear performance. In another case, the same group studied the tribological behavior of nano-LDHs with different sizes [25]. The obtained LDHs with oleylamine could disperse well in base oil to form a stable homogeneous dispersion. As lubricant additives, their tribological performances in base oil were improved both in terms of friction reduction and antiwear performance.

In this work, we chose a coprecipitation method to synthesize LDH nanoplatelets. The relationship between surface functionalization and dispersion efficiency was studied after dispersion in similar base oils. Subsequently, the friction and wear properties of different oil samples were evaluated by ball-on-disk method in reciprocating friction meter mode. Then, their sliding contact surfaces were analyzed and tested to determine whether the tribofilms of specific components led to LDH nanoadditives. Based on these results, the tribological behavior and potential lubrication mechanism of nano-LDH additives are proposed herein.

## 2. Experimental Procedure

### 2.1. Materials

Mg(NO<sub>3</sub>)<sub>2</sub>·6H<sub>2</sub>O, Al(NO<sub>3</sub>)<sub>3</sub>·9H<sub>2</sub>O (analytically pure, >99.0%), NaOH (analytically pure, >96.0%) and Na<sub>2</sub>CO<sub>3</sub> (analytically pure, >99.8%) were used as raw materials (Aladdin, Shanghai, China). Y is Yubase 6, a kind of mineral base oil produced by SK Lubricants GmbH (Seoul, Korea); M is 500SN, a kind of mineral base oil produced by ExxonMobil Chemical (Spring, TX, USA); T is alkyl naphthalene, a kind of synthetic base oil produced by ExxonMobil Chemical; DA1 is a dispersant produced by Lubrizol (Midland, MI, USA); DA2 is a dispersant produced by Chevron (San Ramon, CA, USA); DA3 is a dispersant produced by KKK OLEO (Selangor, Malaysia); and T501 is a kind of antioxidant produced by LANXESS (Cologne, Germany).

### 2.2. Preparation of MgAl LDH Particles

MgAl LDH was synthesized by coprecipitation method. A mixed alkaline solution of NaOH and Na<sub>2</sub>CO<sub>3</sub> ([OH<sup>-</sup>] = 0.8 M) was added dropwise to a stirred mixed salt solution of Mg(NO<sub>3</sub>)<sub>2</sub>·6H<sub>2</sub>O and Al(NO<sub>3</sub>)<sub>3</sub>·9H<sub>2</sub>O with a Mg<sup>2+</sup>/Al<sup>3+</sup> molar ratio of 2:1 ([Mg<sup>2+</sup>] + [Al<sup>3+</sup>] = 0.3 M) at room temperature until the pH reached 10, then stirred for 0.5 h. The resulting suspension was aged for 12 h at 150 °C in an autoclave. After that, the precipitate was filtered and washed several times with distilled water and absolute ethanol until pH = 7 and dried at 60 °C for 12 h.

### 2.3. Preparation of Lubricating Oil Samples

Lubricating oil samples were prepared using the sample preparation method according to the composition listed in Table 1. According to the recipe, the raw materials were added to a transparent beaker and stirred at a constant temperature of 60 °C for 30 min.

**Table 1.** Composition of lubricating oil samples.

Serial Number	Sample Name	Sample Composition, %						
		Y	M	T	LDH	DA1	DA2	DA3
1	Y1	99.4	-	-	0.2	0.2	0.2	-
2	Y2	99.8	-	-	-	0.1	0.1	-
3	Y3	99.85	-	-	0.05	0.05	0.05	-
4	Y4	99.7	-	-	0.10	0.10	0.10	-
5	Y5	99.7	-	-	0.2	-	-	0.1
6	Y6	99.6	-	-	0.2	-	-	0.2
7	Y7	99.3	-	-	0.2	-	-	0.5
8	Y8	99.6	-	-	-	0.2	0.2	-
9	M1	-	99.4	-	0.2	0.2	0.2	-
10	M2	-	99.6	-	-	0.2	0.2	-
11	T1	-	-	99.4	0.2	0.2	0.2	-
12	T2	-	-	99.6	-	0.2	0.2	-

#### 2.4. Characterization of LDH

LDHs were characterized by X-ray diffraction (XRD) with a Rigaku diffractometer ( $\text{CuK}\alpha$  source;  $\lambda = 0.15406$  nm; operated at 40 kV and 100 mA; scanning rate,  $10^\circ \text{ min}^{-1}$  from  $3^\circ$  to  $70^\circ$  ( $2\theta$ )). The crystal plane spacing ( $d$ ) of the diffraction peaks was calculated based on the Bragg equation,

$$n\lambda = 2d_{(hkl)} \sin \theta$$

where  $n$  is an integer,  $hkl$  are crystallographic directions,  $\lambda$  is the known X-ray wavelength (0.15406 nm) and  $\theta$  is the diffraction angle. The Fourier transform infrared (FT-IR) spectrum was recorded using a VERTEX 70v FT-IR spectrometer ( $4000\sim 450 \text{ cm}^{-1}$ , KBr sheet) (Bruker, Bremen, Germany). The morphology of LDHs was observed on a scanning electron microscope (SEM, ZeissSupra 55, Oberkochen, Germany). The metal elementary composition of the LDHs was determined by inductively coupled plasma-atomic emission spectroscopy (ICP-AES, Shimadzu ICPS-7500, Japan).

#### 2.5. Test of Lubricating Oil Samples

The composition of lubricating oil samples was tested by a Spectroil 100 rotary disc electrode atomic emission spectrometer (Q100) (SPECTRO SCIENTIFIC, Chelmsford, MA, USA, test method ASTM D6595). A friction and wear test was performed by an SRV<sup>®</sup>5 multifunctional friction and wear testing machine (Optimol, München, Germany, test method ASTM D5707). The morphology and composition of SRV plates were characterized on a scanning electron microscope (SEM, Zeiss Supra 55, Oberkochen, Germany). The viscosity of lubricating oil samples was determined by a rheometer (TA) with shear rate of 1/s. The antiwear performance of lubricating oil samples was tested by a four-ball machine. The antioxidation of lubricating oil samples was evaluated by an oxidation stability bath (Koehler, RBOT). The total acid value was determined by an automatic potentiometric titrator (Metrohm, Herisau, Switzerland).

After the sample was prepared, the appearance and sedimentation at the bottom of the beaker were observed, and a sample was taken from the middle of the beaker every 24 h. A Q100 elemental analysis instrument was used to test the characteristic elements (Al) to characterize the dispersion effect of different formulation systems in the base oil. Through a four-ball test, the antiwear properties of the samples with different LDH ratios were tested. The viscosity of lubricating oil samples after adding LDH and T501 was compared by rheological test. The fretting wear resistance of different lubricating oil samples was compared by SRV test.

For the SRV test, the friction subsets were steel balls and steel discs, with reference to the ASTM D5707 standard method. Test balls: 52100 steel,  $60 \pm 2$  Rc hardness,  $0.025 \pm 0.005$ - $\mu\text{m}$  Ra surface finish, 10 mm diameter. Lower test disk: 52100 steel,  $60 \pm 2$  Rc hardness. The topography of the disk was determined by four values:  $0.5 \mu\text{m} < \text{Rz} < 0.650 \mu\text{m}$ ;  $0.035 \mu\text{m} < \text{C.L.A.}$ ;

(Ra) < 0.050  $\mu\text{m}$ ;  $0.020 \mu\text{m} < R_{pk} < 0.035 \mu\text{m}$ ; and  $0.050 \mu\text{m} < R_{vk} < 0.075 \mu\text{m}$ , 24 mm diameter by 7.85 mm thick. The wear of the samples was tested by the four-ball machine method, with steel balls at the friction substrate, with reference to the ASTM D2266 standard method. Test balls: chrome alloy steel made from AISI standard steel No. E-52100 with a diameter of 12.7 mm, grade 25 EP (Extra Polish). The Rockwell C hardness was 64 to 66.

For the dispersibility study reported in this paper, 300 mL of lubricant sample was used, with 2 mL used for the elemental test. For the four-ball machine test, 10 mL of lubricant sample was used. For the SRV test, 0.5 mL of lubricant sample was used, while for the rheological measurement, 1 mL of sample was used.

### 3. Results and Discussion

#### 3.1. Characterization of Synthetic Powders

Figure 1 shows the XRD patterns of MgAl LDH synthesized at a crystallization temperature of 150 °C and an aging time of 12 h. All the main diffraction peaks are in good agreement with the features of the hexagonal phase. The (003), (006) and (009) peaks appear at 11.66°, 23.37° and 34.95°, respectively. The (110) peak representing the layered structure appears at 60.47°. The base distance of  $d(003)$  is 0.755 nm, and the base distance of  $d(110)$  is 0.152 nm. Narrow and sharp diffraction peaks indicate that the samples have good crystallinity and no impurities.

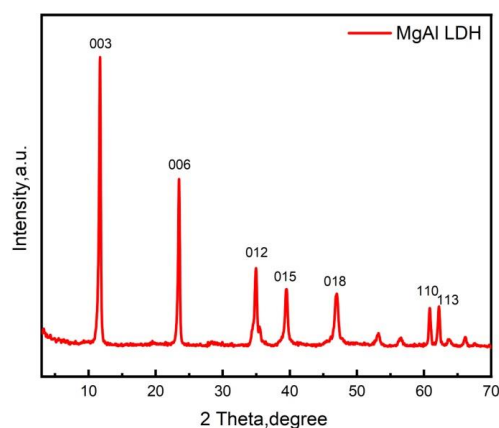


Figure 1. XRD patterns of MgAl LDH.

The SEM image (Figure 2) of the MgAl LDH sample exhibits a typical hydrotalcite hexagonal layered structure and uniform crystal shape and size, with an average disk diameter of about 240 nm.

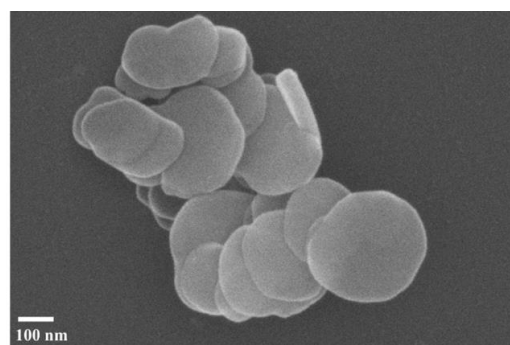
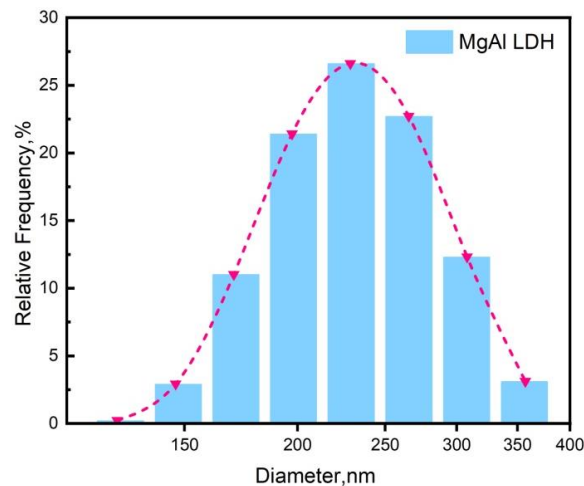


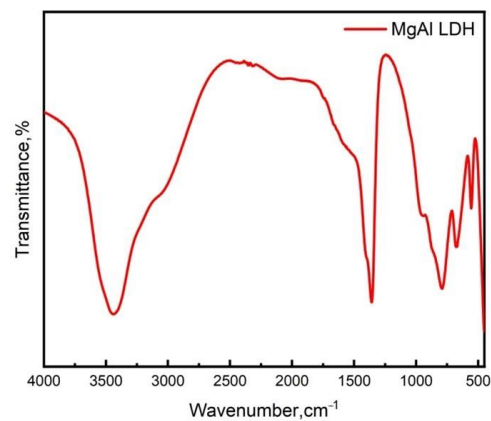
Figure 2. SEM image of MgAl LDH.

Figure 3 shows the average particle size distribution of MgAl LDH nanoparticles. Dashed lines indicate the fitting results of normal distribution, and the median widths of MgAl LDH nanoplatelets are 230 nm, in agreement with the SEM results.



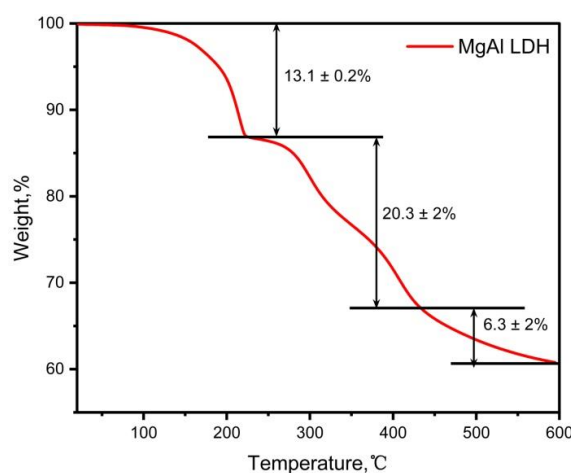
**Figure 3.** Bar graph for the particle size distribution of MgAl LDH. The red line shows the particle size distribution curve obtained by fitting the bar graph.

Figure 4 shows the FT-IR spectroscopies of MgAl LDH; the intense band observed at about  $3445\text{ cm}^{-1}$  is assigned to the OH stretching vibration of water molecular and hydroxyl groups of brucite-like layers. The shoulder around  $3050\text{ cm}^{-1}$  is attributed to hydrogen bonds between interlayer water and  $\text{CO}_3^{2-}$ . The  $\nu_3$  asymmetric stretching vibration frequency of the  $\text{CO}_3^{2-}$  moves to the lower wavenumber of  $1369\text{ cm}^{-1}$ , mainly due to interaction of carbonate anions with interlayer water molecules through hydrogen bonds. The  $\nu_2$  and  $\nu_4$  vibrations of  $\text{CO}_3^{2-}$  correspond to  $943\text{ cm}^{-1}$  and  $677\text{ cm}^{-1}$ , respectively. In addition, the vibrations at about  $796\text{ cm}^{-1}$  and  $553\text{ cm}^{-1}$  can be assigned to the interaction of  $\text{CO}_3^{2-}$  with the brucite-like layers.



**Figure 4.** FT-IR spectrum of MgAl LDH.

Figure 5 illustrates the TGA curves of MgAl LDH. The thermal decomposition processes of MgAl LDH can be divided into three stages. Stage I occurs from room temperature to  $222\text{ }^\circ\text{C}$ , owing to evaporation of moisture adsorbed on the outer surface of the nanoplatelets and water molecules existing in the LDH interlayer channels. The weight losses of MgAl LDH in stage I were  $13.1 \pm 0.2\%$ . ICP results show that the ratio of Mg to Al is around 2:1. In view of the weight loss in stage I, the formula of MgAl LDH can be expressed as  $\text{Mg}_2\text{Al}(\text{OH})_6(\text{CO}_3)_{0.5} \cdot 1.7\text{H}_2\text{O}$ . The variation from  $222$  to  $430\text{ }^\circ\text{C}$  in stage II was attributed to the dehydroxylation of LDH and the release of volatile substances by the interlayer  $\text{CO}_3^{2-}$  anions, with weight losses of  $20.3 \pm 2\%$ . With a further increase in the temperature,  $\text{CO}_3^{2-}$  and hydroxyl were eliminated gradually from the interlayer and the layer structure of MgAl LDH collapsed. In this stage, LDH finally transformed into layered double oxides (LDOs), and the residual weights of MgAl LDH were  $66.9 \pm 2\%$ .



**Figure 5.** TGA curves of MgAl LDH.

### 3.2. Antioxidation of LDH in Base Oil

Tables 2 and 3 show the rotary oxygen bomb test data of different LDHs dispersed in base oil. As can be seen from the table, the oxidation induction time of adding different hydrotalcite samples is longer than that of base oil, and Table 3 shows that the total acid value of base oil increased the most before and after the test. The results show that the oxidation stability of the three samples with LDH is greater than that of base oil. Compared with LDH2 and LDH3, LDH1 has a longer oxidation induction period at the same sample concentration, as shown in Table 3. The total acid value of LDH2 and LDH3 samples changed considerably before and after the rotary oxygen bomb test, while the total acid value of LDH1 only increased by 0.01 mgKOH/g, indicating that the oxidation stability of lubricating oil was most obviously improved when the ratio of Mg:Al was 2:1.

**Table 2.** Different LDHs in base oil.

Sample	Additive Concentration/% (Mass)
Base oil	-
Base oil + LDH1	0.2
Base oil + LDH2	0.2
Base oil + LDH3	0.2

**Table 3.** Antioxidant test data of different LDHs in base oil.

Sample	Total Acid Value before Rotating Oxygen Bomb Test, mgKOH/g	Total Acid Value after Rotating Oxygen Bomb Test, mgKOH/g	Oxidation Induction Time, Min
Base oil	0	3.22	150
Base oil + LDH1	0	0.01	668
Base oil + LDH2	0	0.7	317
Base oil + LDH3	0	0.28	615

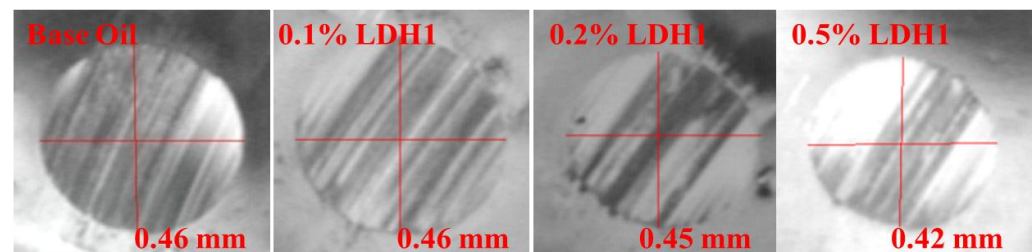
### 3.3. Investigation of Wear Resistance of LDH in Base Oil

Table 4 shows the lubrication performance of lubricating oil samples with 0.1%, 0.2% and 0.5% LDH1. As shown in the table, the wear scar diameters of lubricating oil samples with 0.1% and 0.2% LDH1 concentration were 0.46 mm and 0.45 mm respectively, basically consistent with the wear scar diameter of base oil, failing to effectively reduce surface wear. When the concentration was increased from 0.2% to 0.5%, the wear scar diameter decreased from 0.45 mm to 0.42 mm in the four-ball test; the wear scar diameter decreases by 0.04 mm compared with the base oil, and the friction performance was significantly improved, indicating that the oil has the best lubrication properties when the concentration of LDH is 0.5%. This can be explained by the fact that at a low concentration, it is difficult

to completely cover the metal surface to form an effective protective film. It can also be seen from Figure 6 that the grooves on the wear surface produced by the LDH sample with a concentration of 0.5% are significantly narrower than those of 0.1% and 0.2% and that the wear scars are smaller.

**Table 4.** Wear scar diameter data of samples with different concentrations of LDH1.

Sample	Concentration of Additive/% (Mass)	Four-Ball Test Spot Diameter (mm)
Base Oil	100	0.46
LDH1	0.5	0.42
	0.2	0.45
	0.1	0.46



**Figure 6.** Surface morphology of four spheres of LDH1 samples with different concentrations.

### 3.4. Viscosity–Temperature Characteristics

The rheological properties of lubricating oil with different antioxidants were studied by rheometer (between  $-30\sim 90$ ). Figure 7 shows that the viscosity changes exponentially with temperature. The kinematic viscosity of four types of lubricating oil drops sharply from  $-30$  to  $10$  °C, but at  $10\sim 90$  °C, the curve is relatively flat, and the decrease becomes smaller. In the low-temperature operating range ( $-30\sim 10$  °C), the lubricating oil sample with 0.5% LDH is less cryogenic than the base oil sample; in particular, at  $-28.45$  °C, the dynamic viscosity of the oil sample is  $1.95106$  Pa·s, while the dynamic viscosity of the base oil at this temperature is  $1.51329$  Pa·s. The low-temperature performance of lubricating oil samples with 0.5% LDH1 was similar to that of base oil in the low-temperature working range, indicating that the addition of LDH did not change the low-temperature performance of base oil. The lubricating oil sample with 0.5% T501 had better low-temperature performance than the other three oil samples, and the dynamic viscosity was  $1.10764$  Pa·s at  $-28.45$  °C. In the high-temperature working interval ( $40\sim 90$  °C), the dynamic viscosity of the four oil samples is similar, indicating that the viscosity decline trend of the base oil in the high-temperature working interval with the addition of organic antioxidants and LDH is the same as that after adding three kinds of antioxidant.

Further information was obtained when the viscosity data were fitted to the temperature power law model (Equation (1)).

$$\eta = \eta_0 \left( \frac{T - T_x}{T_x} \right)^{-\gamma} \quad (1)$$

In this model,  $\eta_0$  represents the asymptote value,  $T_x$  is a threshold temperature at which the sample becomes fragile and  $\gamma$  is the parameter that modulates the effect of the temperature on the viscosity. This model allowed us to construct a master curve using the relative viscosity ( $\eta_r$ ) and relative temperature ( $T_r$ ), as described by Equations (2) and (3), respectively.

$$\eta_r = \left( \frac{\eta}{\eta_0} \right)^{-1/\gamma} \quad (2)$$

$$T_r = \frac{T}{T_x} \quad (3)$$

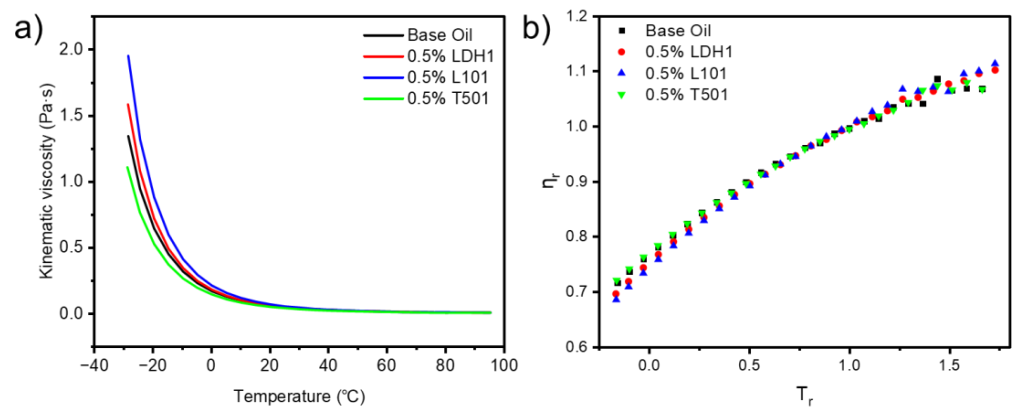


**Figure 7.** (a) Temperature dependence of viscosity and (b) master curves for different antioxidant samples.

The master curves are shown in Figure 7b and summarized in Table 5. It is clearly seen that the addition of T501 and L101 causes a deviation in the model. Since T501 and L101 reduce the effect of temperature on the viscosity of the lubricant, this deviation of the master curves occurred when the temperature was raised. In the case of LDH, the master curve is in good agreement with the model.

**Table 5.** Power law fitting parameters for different antioxidant samples.

Power Law	$\eta_0$ (Pa · s)	$T_x$ (K)	$\gamma$	$R^2$
Base Oil	0.01962	122.306	12.65872	0.99856
0.5%LDH1	0.02081	117.743	11.96237	0.9984
0.5%L101	0.02365	117.779	11.67762	0.99832
0.5%T501	0.01569	122.261	12.99526	0.99835

### 3.5. Study of Dispersibility of LDH Material-Dispersant Systems in Different Lubricating Oils

The composition of the Y1 sample was 0.2% oleylamine, 0.2% calcium salicylate and 0.2% LDH, with the remainder composed of Yubase 6. The composition of the M1 sample was 0.2% oleylamine, 0.2% calcium salicylate and 0.2% LDH, with the remainder composed of Mobil 500 SN. The composition of the T1 sample was 0.2% oleylamine, 0.2% calcium salicylate and 0.2% LDH, with the remainder composed of alkyl naphthalene. Figure 8 shows the variation in Al and Mg elemental content in the samples containing different types of base oils over time; the dispersion performance of the same dispersant system in different base oils for LDH was also investigated. On the first day after sample preparation, the contents of Al and Mg elements in Y1, M1 and T1 samples were 59 ppm and 113 ppm, 73 ppm and 143 ppm, and 38 ppm and 70 ppm, respectively. From the calculation, the theoretical content of Al elements in the samples was 115 ppm. After LDH and the dispersant system were added to the base oil, sedimentation occurred rapidly, and after one day, the LDH content in the M1 sample was the highest, reaching 63.5% of the added amount, that in the Y1 sample was the second highest and that in the T1 sample was the lowest, at only 33% of the added amount. With the extension of time, the elemental Al in the samples showed a decreasing trend. After 56 days, it leveled off, with the highest Al content of 11 ppm in the M1 sample dropping to 9.6% of the added amount and the lowest content of 2.6 ppm in the T1 sample almost completely precipitating.

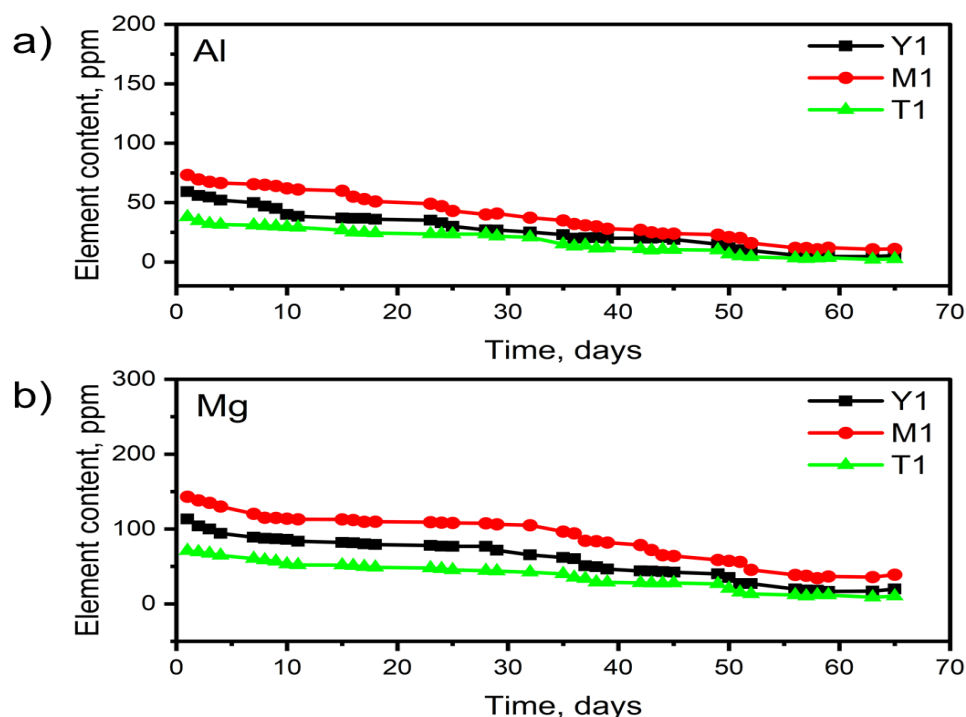


**Figure 8.** Curve of (a) Al and (b) Mg elemental content over time in samples Y1, M1 and T1.

Figure 8 show that the same LDH and dispersant system has different dispersion performance in different base oils, with the best performance in base oil M and the worst in base oil T. After 30 days of storage in lab environment (room-temperature:  $\sim 25\text{ }^{\circ}\text{C}$ , relative humidity: 30%~70%), the elemental Al content in sample M1 was 40 ppm, and the corresponding LDH content was still 34.7% of the added amount. The viscosity data of base oils Y, M and T are shown in Table 6, with M having the highest viscosity and T having the lowest viscosity. Therefore, it can be concluded that the dispersion performance of LDH in base oil is related to the viscosity of the base oil; the greater the viscosity, the better the dispersion performance and the less likely to sink.

**Table 6.** Data of different base oils.

Item	Y	M	T	Test Method
Kinematic viscosity 40 $^{\circ}\text{C}$ , $\text{mm s}^{-2}$	35.50	93.22	28.38	ASTM D445
Kinematic viscosity 100 $^{\circ}\text{C}$ , $\text{mm s}^{-2}$	6.396	10.64	4.765	ASTM D445
Viscosity index	133	97	79	ASTM D227

### 3.6. Study of the Dispersibility of LDH Dispersant Systems in the Same Lubricating Oil

Figure 9 shows the variation in Al elements in the samples with different amounts of LDH and dispersant added over time, showing the effect of dispersant and LDH addition on the dispersion performance of LDH in the same base oil.

The composition of the Y2 sample was 0.1% oleylamine and 0.1% calcium salicylate, with the remainder composed of Yubase 6. Figure 9 shows that the two dispersant systems have no magnesium and aluminum elements, so Y2 after two months of testing, the magnesium and aluminum elemental contents were zero. The composition of the Y3 sample was 0.05% oleylamine, 0.05% calcium salicylate and 0.05% LDH, with the remainder composed of Yubase 6. Figure 9 shows that the magnesium content of the system tested in the first four days was 43.06 ppm, 38.00 ppm, 35.00 ppm and 32.22 ppm, and the aluminum content was 10.70 ppm, 9.50 ppm, 8.50 ppm and 7.94 ppm, respectively; the magnesium and aluminum contents of the system slowly settled to 13.59 ppm and 2.50 ppm, respectively. The composition of the Y4 sample was 0.1% oleylamine, 0.1% calcium salicylate and 0.1%

of LDH, with the remainder composed of Yubase 6. Figure 9 shows that the magnesium content of the tested system was 105.79 ppm, 98.00 ppm, 90.00 ppm and 75.81 ppm, and the aluminum content was 28.43 ppm, 27.00 ppm, 25.00 ppm and 21.75 ppm for the first four days of testing. After 67 days, the magnesium and aluminum contents of this system settled rapidly to 9.3 ppm and 1.3 ppm, respectively. The composition of the Y1 sample was 0.2% oleylamine, 0.2% calcium salicylate and 0.2% LDH, with the remainder composed of Yubase 6. Figure 9 shows that the magnesium content of the tested system was 118.54 ppm, 112.00 ppm, 105.00 ppm and 97.41 ppm, and the aluminum content was 30.99 ppm, 29.50 ppm, 29.00 ppm and 27.5 0 ppm in the first four days of testing. The magnesium and aluminum contents rapidly settled to 8.97 ppm and 2.02 ppm, respectively after 67 days. A comparison among the magnesium and aluminum contents of samples Y1, Y3 and Y4 in the first four days of testing shows that settling rate in the Y3 and Y4 systems was proportionally correlated with the LDH content, whereas in the Y1 system, the LDH settling rate was faster, with a large deviation between the settling ratio and the amount of addition. From the sixth to seventh day in sample Y3, magnesium and aluminum elements slowly settled, almost reaching an equilibrium, while after the sixth day in samples Y1 and Y4, magnesium and aluminum contents rapidly settled, indicating that with an increase in the proportion of LDH, an equal proportional increase in electric neutral dispersant was unable to delay LDH settling. In particular, after adding more than 0.1% LDH, the electric neutral dispersant was unable to stabilize LDH in the oil phase for a certain period of time. In this study, the LDH structural particle size remained unchanged, and the LDH was positively charged; therefore, the introduction of anionic dispersant needs to be considered.

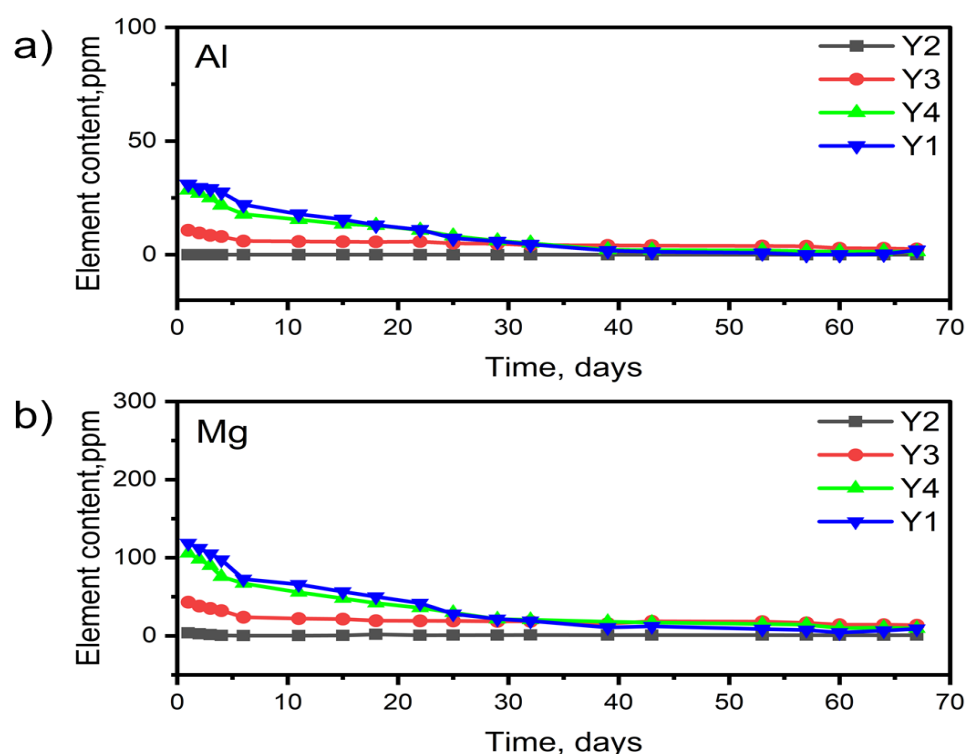


**Figure 9.** Curve of (a) Al and (b) Mg elemental content over time in samples Y1, Y2, Y3 and Y4.

### 3.7. Dispersion of Dispersants to LDH in the Same Lubricating Oil

Figure 10 shows the variation in Al elements in the samples containing different amounts of DA3 dispersant over time, demonstrating the effect of DA3 dispersant content on the dispersion performance of LDH in Y base oil.

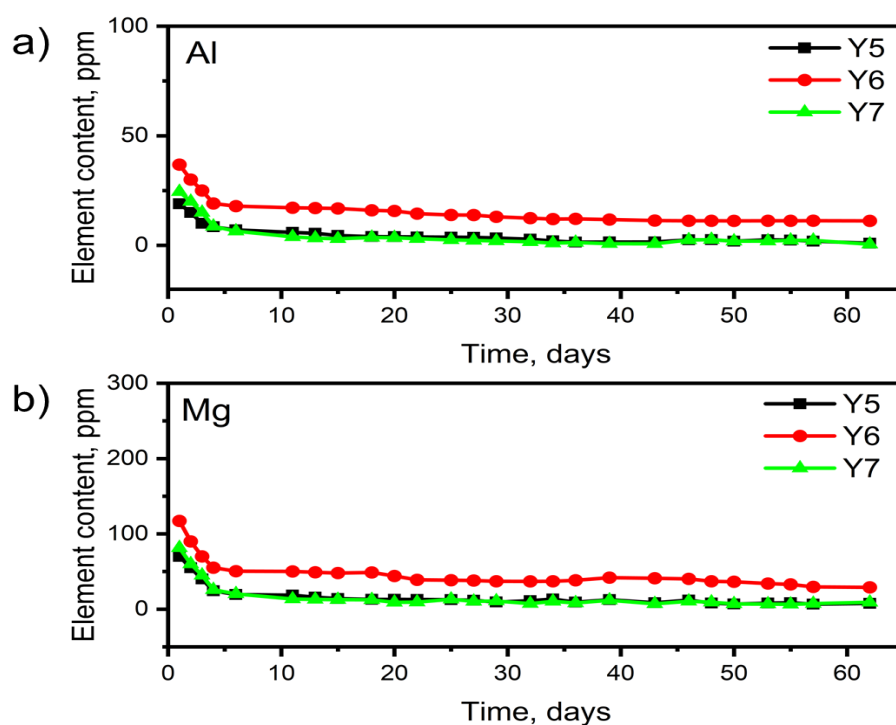
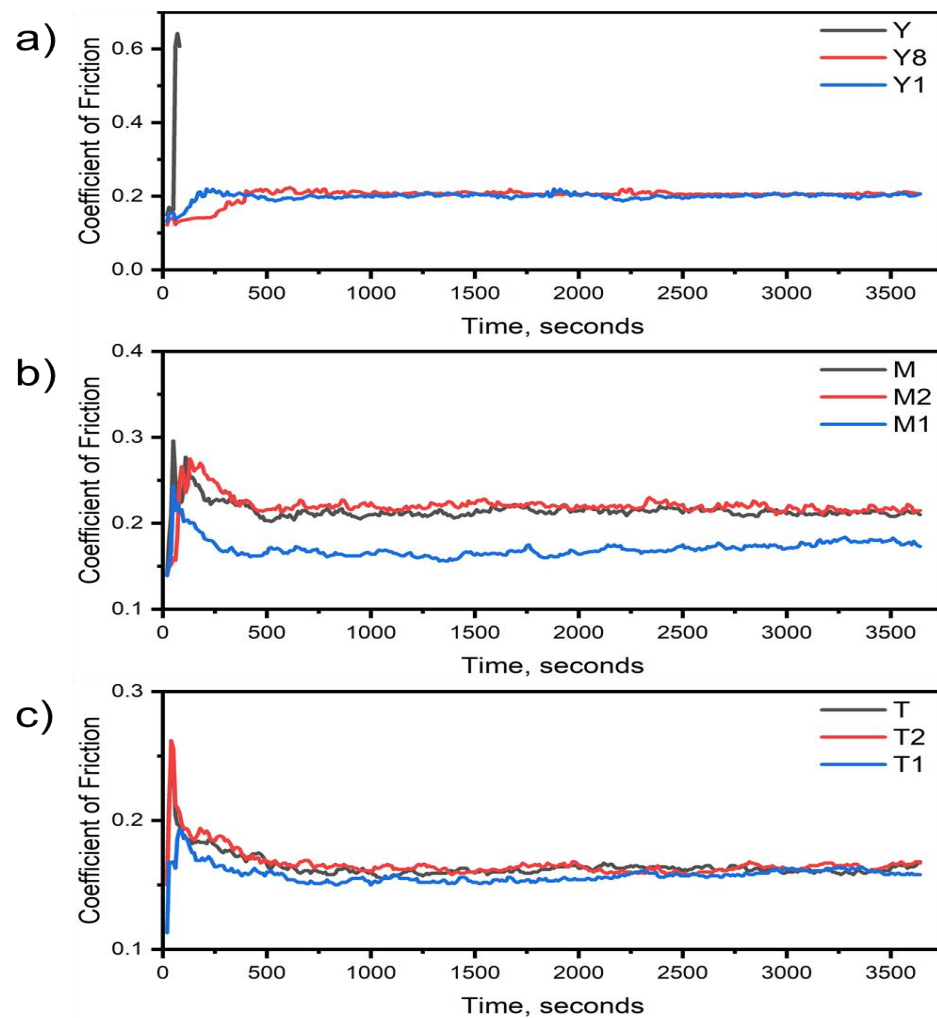


Figure 10. Curve of (a) Al and (b) Mg elemental content over time in samples Y5, Y6 and Y7.

The amounts of LDH addition in Y5, Y6 and Y7 were all 0.2%, and the amounts of DA3 dispersant addition were 0.1%, 0.2% and 0.5%, respectively. On the first day after sample preparation, the contents of Al and Mg in Y6 were 37 ppm and 117.2 ppm, respectively, accounting for 32.2% of the added amount, which is the highest among the three samples. With the extension of time, both Al and Mg elements in the samples gradually decreased and reached a stable value after 34 days; the stable content was basically the same as that in Y1. Figure 10 shows that the highest content of Al elements in the samples, i.e., the highest content of LDH, the least sedimentation and the best dispersion effect when the content of DA3, was 0.2%. DA3 is an anionic dispersant with negative charge, and LDH has a positive charge; therefore, a stable system can be obtained when the two reach charge balance. For a certain amount of LDH, a corresponding amount of DA3 dispersant is required to obtain a system in equilibrium. Therefore, the amount of DA3 dispersant has a great influence on the dispersion performance of LDH, and matching the right amount has a better dispersion effect.

### 3.8. Study on the Wear Resistance of LDH Dispersant Systems in Different Lubricating Oils

As shown in Table 1, the fretting wear resistance of LDH and dispersant systems in different base oils was investigated [11]. An SRV testing machine was used to test the antifretting wear performance of the sample under the following test conditions: load, 200 N; frequency, 50 Hz; amplitude, 1 mm; time, 2 h; temperature, 80 °C. Test conditions: load, 100 N; frequency, 40 Hz; amplitude, 1 mm; time, 1 h; temperature, 40 °C. The results are shown in Figures 11 and 12. With Y as the base oil, the SRV curve suddenly increases at the initial time, the test fails and obvious abrasions occur on the contact surface. With the addition of the dispersant sample, SRV performance was virtually improved, and the test failed. Y1 samples of dispersants and LDH materials were added, and the SRV test was passed with a smooth relative coefficient of friction and no abrasions. As a result, LDH improved the fretting wear resistance of the lubricants.



**Figure 11.** SRV friction coefficient for samples (a) Yubase 6, (b) 500S N and (c) alkyl naphthalene base oils under 100 N.

Figure 12 shows that when the loading was reduced in the SRV test, the frequency and temperature were reduced under the following test conditions: load, 200 N; frequency, 40 Hz; amplitude, 1mm; time, 1 h; and temperature, 40 °C. Except for the base oil Y, the SRV of other samples passed the test, but with different friction coefficients. In Yubase 6, the coefficient of friction of the SRV was almost constant when LDH was added. In 500 SN, the SRV coefficient of friction was reduced from 0.22 to 0.17 with the addition of LDH material. In alkyl naphthalene, the coefficient of friction of the SRV was almost constant when LDH was added. Compared to the three base oils, the coefficient of friction of the alkyl naphthalene sample was lower than that of Yubase 6 and 500 SN. As a result, LDH materials significantly reduced the friction coefficient in 500SN base oils and significantly improved the fretting resistance of the lubricants.

### 3.9. Antiwear Performance of LDH Dispersant System in the Same Lubricating Oil

An SRV tester was used to test the antifretting wear performance of the sample under the following conditions: frequency, 40 Hz; amplitude, 1mm; time, 1 h; temperature, 40 °C; load, 100 N. The antiwear properties of different dispersion systems in the same base oil were examined. Figure 13 shows that the coefficient of friction of the sample was significantly reduced after increasing the content of LDH and dispersant in the same base oil. The change in wear resistance over time was investigated. Figure 14 shows that for Y1 samples, the coefficient of friction did not change much within 49 days, and the antiwear performance of LDH in lubricating oil was relatively stable.

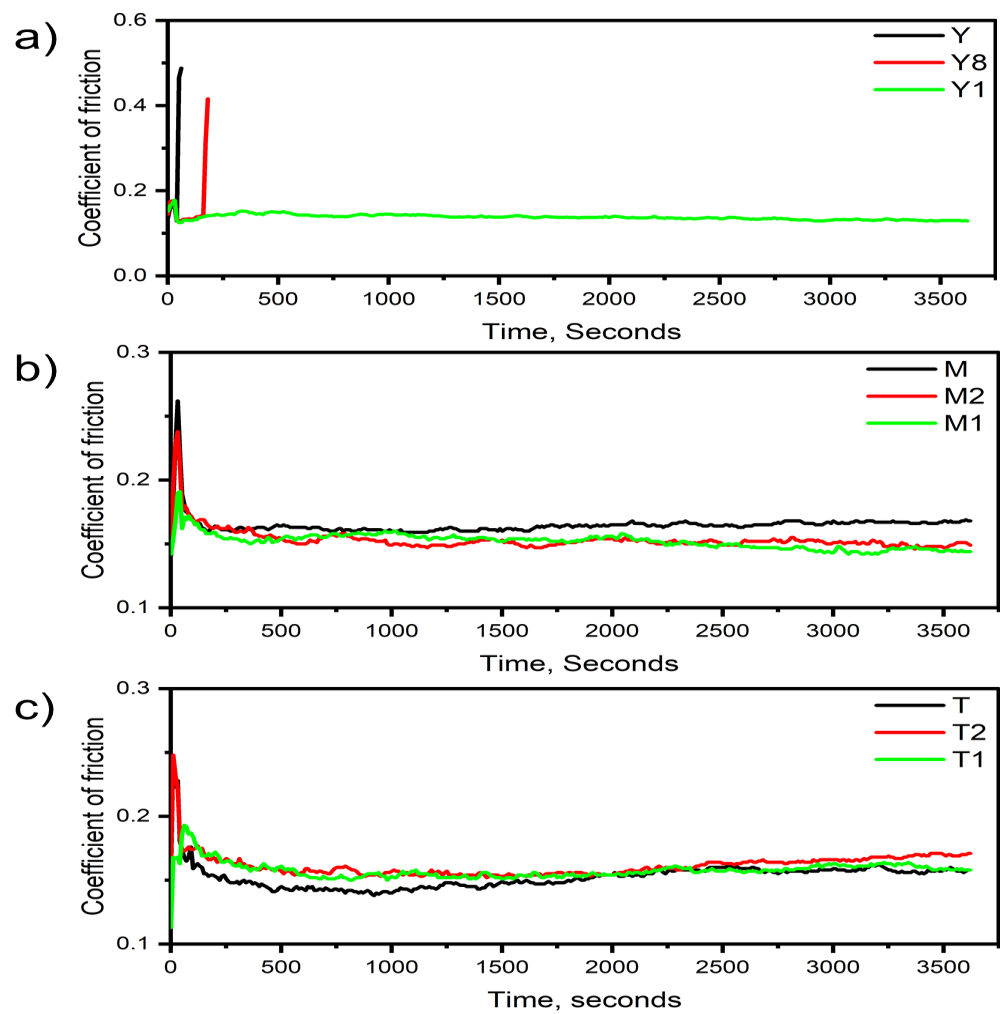


Figure 12. SRV friction coefficient for samples (a) Yubase 6, (b) 500S N and (c) alkyl naphthalene base oils under 200 N.

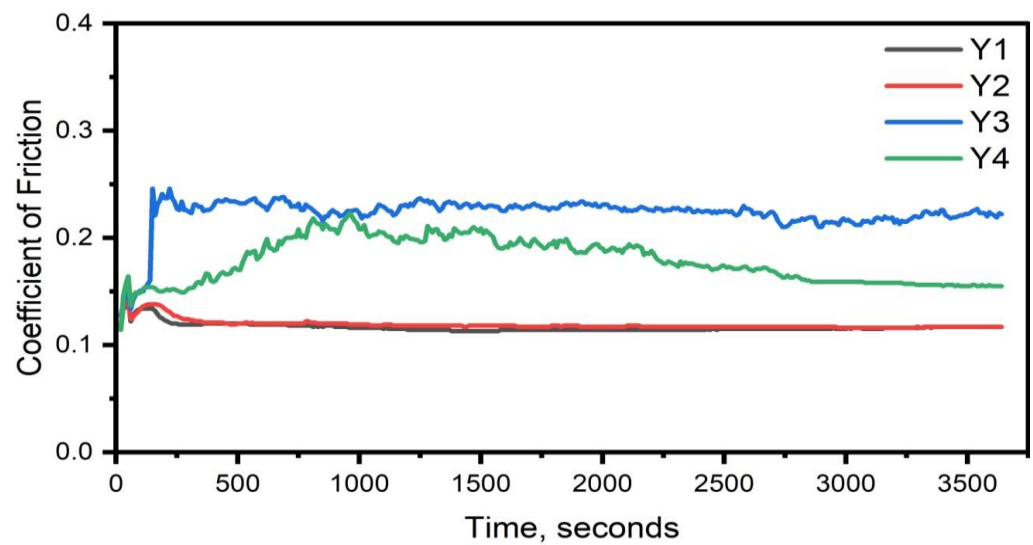
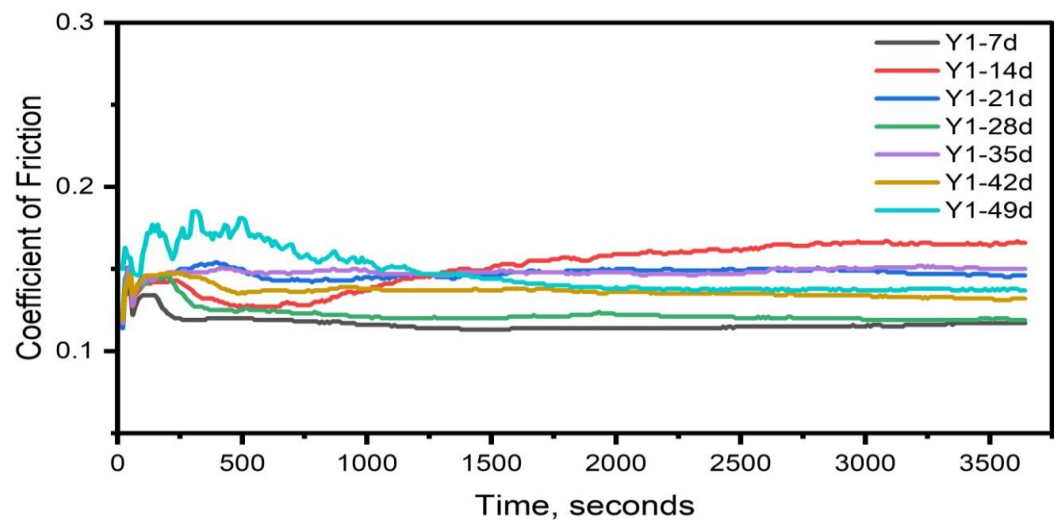
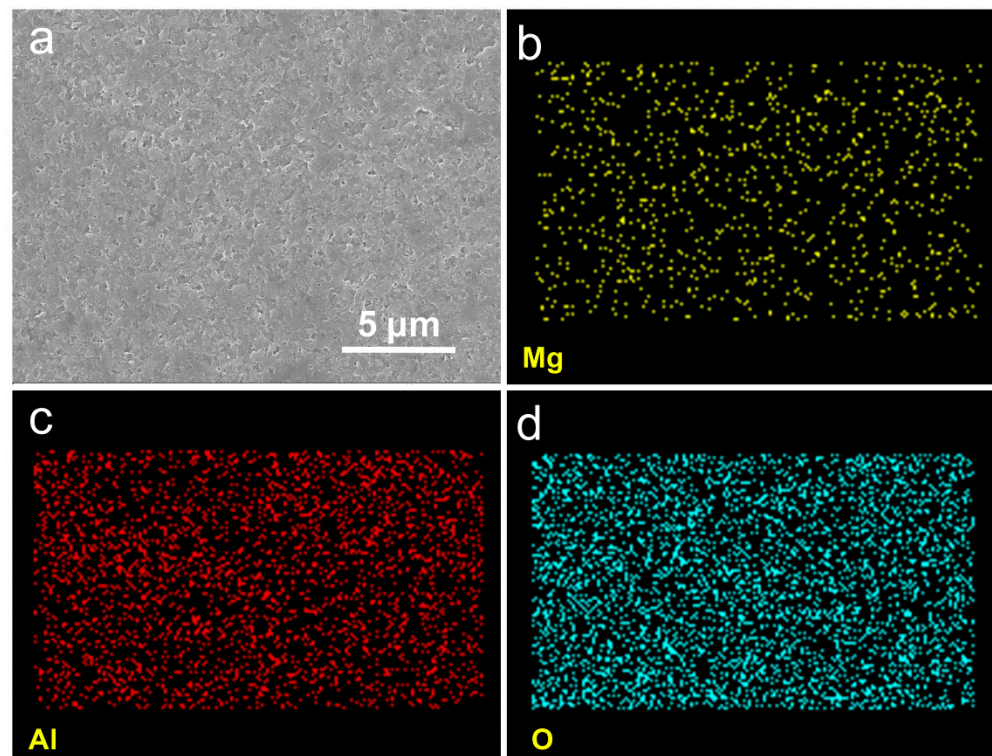


Figure 13. SRV friction coefficient for samples Y1, Y2, Y3 and Y4 under 100 N.



**Figure 14.** SRV friction coefficient for sample Y1 under 100 N after settling different times.

The wear scars on the steel plate after the SRV test were characterized by SEM. The morphology and composition are shown in Figure 15. Before the SRV test, the surface of the steel plate was not smooth and had no characteristic elements. After the SRV test, Al, Mg and O elements were observed on the surface of the steel plate, which are the characteristic elements of LDH. A uniform and dense protective film was formed, which reduced the friction coefficient and wear in the SRV test. Based on EDS surface analysis to understand the lubrication mechanism, with LDH deposition on the contact interface, LDH nanosheets can enter into the defects and pits of the sliding surface to form a dense friction film and avoid direct contact with the loaded surface. The reason for the lower friction coefficient for nanosheets with higher dispersion is that the better the dispersion, the more easily the LDH nanosheets can enter into the contact interface, which is important for tribological applications.



**Figure 15.** (a) SEM image and EDS results of the SRV platters: (b) Mg, (c) Al and (d) O elements.

#### 4. Conclusions

(1) LDH and dispersant systems vary greatly in terms of dispersibility between different base oils, with the best dispersion in 500 SN and the worst dispersion in alkyl naphthalene.

(2) Selecting a suitable dispersant, such as DA3, can significantly improve the dispersion performance of LDH in Yubase 6 base oils. After 32 days, the active element content of LDH was still 40%, while other dispersant systems had less than 10% element content. After increasing the dispersant content, the dispersion effect was not significantly improved.

(3) LDH significantly reduced the coefficient of friction and significantly improved the fretting wear resistance of lubricants via the formation of a uniform and dense film on the friction surface. With an increase in time, the coefficient of friction did not change much, and the antiwear performance of LDH in lubricating oil was relatively stable.

**Author Contributions:** Conceptualization, Y.L. and J.H.; methodology, Y.L. and W.Z.; software, W.Z. and Y.H.; validation, Q.Z., W.Z. and Y.H.; formal analysis, Y.L.; investigation, Y.L., W.Z. and Y.H.; resources, Y.L.; data curation, Q.Z. and W.Z.; writing—original draft preparation, Y.L. and Q.Z.; writing—review and editing, W.Z.; visualization, W.Z.; supervision, J.H.; project administration, J.H.; funding acquisition, J.H. All authors have read and agreed to the published version of the manuscript.

**Funding:** This work was supported by the National Natural Science Foundation of China (21671015), the Fundamental Research Funds for the Central Universities (BHYC1702B).

**Data Availability Statement:** The data that support the findings of this study are available from the corresponding author.

**Conflicts of Interest:** The authors declare no conflict of interest.

#### References

1. Peña-Parás, L.; Taha-Tijerina, J.; Garza, L.; Maldonado-Cortés, D.; Michalczewski, R.; Lapray, C. Effect of CuO and Al<sub>2</sub>O<sub>3</sub> nanoparticle additives on the tribological behavior of fully formulated oils. *Wear* **2015**, *332–333*, 1256–1261. [[CrossRef](#)]
2. Cox, P.M.; Betts, R.A.; Jones, C.D.; Spall, S.A.; Totterdell, I.J. Acceleration of Global Warming due to Carbon-Cycle Feedbacks in a Coupled Climate Model. *Nature* **2000**, *408*, 184–187. [[CrossRef](#)]
3. Fontaras, G.; Samaras, Z. On the Way to 130 G CO<sub>2</sub>/Km Estimating the Future Characteristics of the Average European Passenger Car. *Energy Policy* **2010**, *38*, 1826–1833. [[CrossRef](#)]
4. Gong, Z.; Jia, X.; Ma, W.; Zhang, B.; Zhang, J. Hierarchical structure graphitic-like/MoS<sub>2</sub> film as superlubricity material. *Appl. Surf. Sci.* **2017**, *413*, 381–386. [[CrossRef](#)]
5. Ahmadijokani, F.; Shojaei, A.; Arjmand, M.; Alaei, Y.; Yan, N. Effect of short carbon fiber on thermal, mechanical and tribological behavior of phenolic-based brake friction materials. *Compos. Part B Eng.* **2019**, *168*, 98–105. [[CrossRef](#)]
6. Holmberg, K.; Erdemir, A. Influence of tribology on global energy consumption, costs and emissions. *Friction* **2017**, *5*, 263–284. [[CrossRef](#)]
7. Zhang, Y.; Sun, J.; Zheng, Y.; Ge, X.; Peng, X.; Hong, Y.; Fernandez-Rodriguez, E. Unsteady characteristics of lubricating oil in thrust bearing tank under different rotational speeds in pumped storage power station. *Renew. Energy* **2022**, *201*, 904–915. [[CrossRef](#)]
8. Domínguez-García, S.; Maya-Yescas, R.; Béjar-Gómez, L. Reduction of lubricant life in lubrication systems for internal combustion engines due to high lubricant supply rates. *Mater. Lett.* **2022**, *313*, 131785. [[CrossRef](#)]
9. Chen, S.; Wu, T.; Zhao, C. Synthesis of Branched Biolubricant Base Oil from Oleic Acid. *ChemSusChem* **2020**, *13*, 5516–5522. [[CrossRef](#)]
10. Mubashshir, M.; Shaikat, A. The Role of Grease Composition and Rheology in Elastohydrodynamic Lubrication. *Tribol. Lett.* **2019**, *67*, 104. [[CrossRef](#)]
11. Kumari, S.; Sharma, O.P.; Khatri, O.P. Alkylamine-functionalized hexagonal boron nitride nanoplatelets as a novel material for the reduction of friction and wear. *Phys. Chem. Chem. Phys.* **2016**, *18*, 22879–22888. [[CrossRef](#)] [[PubMed](#)]
12. Feng, P.; Ren, Y.; Li, Y.; He, J.; Zhao, Z.; Ma, X.; Fan, X.; Zhu, M. Synergistic lubrication of few-layer Ti<sub>3</sub>C<sub>2</sub>T<sub>x</sub>/MoS<sub>2</sub> heterojunction as a lubricant additive. *Friction* **2022**, *10*, 2018–2032. [[CrossRef](#)]
13. Xu, Z.; Lou, W.; Zhao, G.; Zheng, D.; Hao, J.; Wang, X. Cu nanoparticles decorated WS<sub>2</sub> nanosheets as a lubricant additive for enhanced tribological performance. *RSC Adv.* **2019**, *9*, 7786–7794. [[CrossRef](#)]
14. Paul, G.; Hirani, H.; Kuila, T.; Murmu, N.C. Nanolubricants dispersed with graphene and its derivatives: An assessment and review of the tribological performance. *Nanoscale* **2019**, *11*, 3458–3483. [[CrossRef](#)] [[PubMed](#)]
15. Yang, Y.; Fan, X.; Yue, Z.; Li, W.; Li, H.; Zhu, M. Synergistic lubrication mechanisms of molybdenum disulfide film under graphene-oil lubricated conditions. *Appl. Surf. Sci.* **2022**, *598*, 153845. [[CrossRef](#)]

16. Lee, H.; Lee, N.; Seo, Y.; Eom, J.; Lee, S. Comparison of frictional forces on graphene and graphite. *Nanotechnology* **2009**, *20*, 325701. [[CrossRef](#)]
17. Zhao, Y.; Geng, Z.; Li, D.; Wang, L.; Lu, Z.; Zhang, G. An investigation on the tribological properties of graphene and ZDDP as additives in PAO4 oil. *Diam. Relat. Mater.* **2021**, *120*, 108635. [[CrossRef](#)]
18. Zhang, Y.; Xu, H.; Lu, S. Preparation and application of layered double hydroxide nanosheets. *RSC Adv.* **2021**, *11*, 24254–24281. [[CrossRef](#)]
19. Xu, W.; Wang, S.; Li, A.; Wang, X. Synthesis of aminopropyltriethoxysilane grafted/tripolyphosphate intercalated ZnAl LDHs and their performance in the flame retardancy and smoke suppression of polyurethane elastomer. *RSC Adv.* **2016**, *6*, 48189–48198. [[CrossRef](#)]
20. Dragoi, B.; Uritu, C.M.; Agrigoroaie, L.; Lutic, D.; Hulea, V.; Postole, G.; Coroaba, A.; Carasevici, E. MnAl-Layered Double Hydroxide Nanosheets Infused with Fluorouracil for Cancer Diagnosis and Therapy. *ACS Appl. Nano Mater.* **2021**, *4*, 2061–2075. [[CrossRef](#)]
21. Jiang, Y.; Yang, Z.; Su, Q.; Chen, L.; Wu, J.; Meng, J. Preparation of Magnesium-Aluminum Hydrotalcite by Mechanochemical Method and Its Application as Heat Stabilizer in poly(vinyl chloride). *Materials* **2020**, *13*, 5223. [[CrossRef](#)]
22. Evans, D.G.; Duan, X. Preparation of Layered Double Hydroxides and Their Applications as Additives in Polymers, as Precursors to Magnetic Materials and in Biology and Medicine. *Chem. Commun.* **2006**, *5*, 485–496. [[CrossRef](#)]
23. Wang, H.; Liu, Y.; Chen, Z.; Wu, B.; Xu, S.; Luo, J. Layered Double Hydroxide Nanoplatelets with Excellent Tribological Properties under High Contact Pressure as Water-Based Lubricant Additives. *Sci. Rep.* **2016**, *6*, 22748. [[CrossRef](#)]
24. Kutlu, B.; Leuteritz, A.; Boldt, R.; Jehnichen, D.; Heinrich, G. Effects of LDH synthesis and modification on the exfoliation and introduction of a robust anion-exchange procedure. *Chem. Eng. J.* **2014**, *243*, 394–404. [[CrossRef](#)]
25. Wang, H.; Liu, Y.; Liu, W.; Wang, R.; Wen, J.; Sheng, H.; Peng, J.; Erdemir, A.; Luo, J. Tribological Behavior of NiAl-Layered Double Hydroxide Nanoplatelets as Oil-Based Lubricant Additives. *ACS Appl. Mater. Interfaces* **2017**, *9*, 30891–30899. [[CrossRef](#)] [[PubMed](#)]
26. Zhao, D.; Bai, Z.; Zhao, F. Preparation of Mg/Al-LDHs intercalated with dodecanoic acid and investigation of its antiwear ability. *Mater. Res. Bull.* **2012**, *47*, 3670–3675. [[CrossRef](#)]
27. Wang, H.; Wang, Y.; Liu, Y.; Zhao, J.; Li, J.; Wang, Q.; Luo, J. Tribological behavior of layered double hydroxides with various chemical compositions and morphologies as grease additives. *Friction* **2020**, *9*, 952–962. [[CrossRef](#)]

**Disclaimer/Publisher's Note:** The statements, opinions and data contained in all publications are solely those of the individual author(s) and contributor(s) and not of MDPI and/or the editor(s). MDPI and/or the editor(s) disclaim responsibility for any injury to people or property resulting from any ideas, methods, instructions or products referred to in the content.